Ultramicroscopy 184 (2018) 98–105

Contents lists available at ScienceDirect

Ultramicroscopy

journal homepage: www.elsevier.com/locate/ultramic

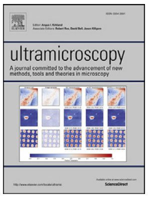

Towards atomically resolved EELS elemental and fine structure mapping via multi-frame and energy-offset correction spectroscopy

Yi Wang*, Michael R.S. Huang, Ute Salzberger, Kersten Hahn, Wilfried Sigle, Peter A. van Aken

Stuttgart Center for Electron Microscopy, Max Planck Institute for Solid State Research, Heisenbergstr. 1, Stuttgart, 70569 Germany

ARTICLE INFO

Article history:
Received 30 March 2017
Revised 16 October 2017
Accepted 20 October 2017
Available online 21 October 2017

Keywords:
STEM
Spectrum image
EELS
Core loss fine structures
Mapping at high resolution

ABSTRACT

Electron energy-loss spectroscopy and energy-dispersive X-ray spectroscopy are two of the most common means for chemical analysis in the scanning transmission electron microscope. The marked progress of the instrumentation hardware has made chemical analysis at atomic resolution readily possible nowadays. However, the acquisition and interpretation of atomically resolved spectra can still be problematic due to image distortions and poor signal-to-noise ratio of the spectra, especially for investigation of energy-loss near-edge fine structures. By combining multi-frame spectrum imaging and automatic energy-offset correction, we developed a spectrum imaging technique implemented into customized DigitalMicrograph scripts for suppressing image distortions and improving the signal-to-noise ratio. With practical examples, i.e. $SrTiO_3$ bulk material and Sr-doped La_2CuO_4 superlattices, we demonstrate the improvement of elemental mapping and the EELS spectrum quality, which opens up new possibilities for atomically resolved EELS fine structure mapping.

1. Introduction

Besides conventional sample imaging, an important capability of modern scanning transmission electron microscopy (STEM) is its integration with microanalysis techniques, such as electron energy loss spectroscopy (EELS) and energy-dispersive X-ray spectroscopy (EDXS). In these analytical techniques, a focused electron probe scans over the sample and at each spatial pixel an imaging signal, i.e. annular dark filed (ADF) or high-angle ADF (HAADF), and analytical signals can be acquired simultaneously. The analytical signals are stored in a dataset referred to as a spectrum image (SI) [1]. With post spectral processing, the SI can be used to create compositional maps, phase maps, or maps of variations in electronic structure. The combination of spatial and spectral information in a single dataset opens up a wide range of data analysis possibilities and provides a powerful tool for material characterization. With the advent of aberration correctors, monochromators, better detectors and cameras, as well as more stable electron optics, sample holder and instrument environments, it is becoming easier to probe materials composition at atomic resolution using STEM spectrum imaging. Despite these improvements, the acquisition and interpretation of atomically resolved EELS and EDXS datasets remain problematic due to image distortions and poor signal-to-noise ratio (SNR) of each individual spectrum constituting the SI, which is mostly due to the small inelastic scattering cross sections that lead to weak signals and long acquisition times. The accessible solutions to these two issues compete with one another. On the one hand, to achieve an acceptable SNR, STEM spectrum imaging generally requires a much higher electron dose than STEM imaging. As a consequence, typical analytical spectrum imaging (EELS and EDXS) dwell times are much longer (1 ms – 10 s) than the ADF dwell times (1 – 50 µs) [2–4]. Higher electron dose can be achieved through either increasing the electron beam current or increasing the dwell time. Increasing the beam current leads to an increase of the probe size; this will reduce the spatial resolution. So this method is of limited use if one wishes to retain atomic resolution. Furthermore, higher beam currents increase potential radiation damage of the sample. On the other hand, increasing the dose through longer acquisition time will increase image distortions caused by time-dependent instabilities of the sample and the microscope. These instabilities may be negligible at lower magnification, but at the level of atomic resolution, instabilities combined with long dwell times may create substantial image distortions. These distortions may prohibit atomic resolution and also limit the interpretability of the SI. Currently, the popular atomic

---

* Corresponding author.
E-mail address: y.wang@fkf.mpg.de (Y. Wang).

https://doi.org/10.1016/j.ultramic.2017.10.014

resolution STEM SI acquisition techniques are using online drift-correction [5,6] or post-acquisition distortion correction [7], or directly summing multiple fast dwell time SIs that have been drift-corrected between separate SI [8]. More recently, rigid and non-rigid registration techniques aligning the multi-frame SI have also been reported [4,9,10].

Among the analytical tools, EELS also provides information of the chemical state because of its high energy resolution. The fine structure in core-loss spectra reflects the local density of unoccupied electron states. Thus, fine structure mapping principally is mapping of the electronic structure of the investigated material [11]. It is well known that EELS SIs usually contain artifacts that compromise the quality of the spectra and these artifacts occur under all circumstances, whether the EELS of a specimen or only a vacuum signal is measured. These artifacts are outlying spectral values (or X-ray spikes), artifacts related to incomplete correction of detector gain and dark current, and shot noise (Poisson noise) whose intensity solely depends on counting statistics. At the present stage, correction of these artifacts is generally done using automated software routines. Gain and dark current references are automatically acquired and applied; outlying spectral values can be removed by replacing them with local median values and shot noise can be minimized by acquiring more electrons, i.e. increasing the beam current, increasing acquisition time, and summing frames. However, as demonstrated by Bosman and Keast [12], automated dark current and gain correction will result in systematic, i.e. correlated noise and impose significant limitations on the quality of EELS. Using an energy-offset correction method, the correlated noise can be efficiently suppressed and allows detection of very weak signals [12–14].

In this work, we report a simple, reliable, and step-by-step spectrum imaging technique to improve the atomically resolved EELS elemental and fine structure mapping quality by combining multi-frame SI with automatic energy-offset correction spectroscopy. Using practical examples, i.e. $SrTiO_3$ bulk material and Sr-doped La_2CuO_4 superlattices, we demonstrate the improvement of elemental mapping and of EELS spectrum quality as well as the possibility of atomically resolved EELS fine structure mapping.

2. Methods

2.1. Multi-frame SI acquisition, energy-offset correction and its reliability

The acquisition of multi-frame SI is realized by a scripting-controlled SI user interface (the SI floating palette) [15,16]. The scripts were developed using DM scripting based on GMS 2.x, which works for line scans as well as for 2D mapping, both for EELS and other simultaneous signals, i.e. EDXS. The script enables to repeatedly acquire a desired number of SIs, where optionally between each SI acquisition spatial drift-correction can be performed and a pre-defined energy-offset is applied to the next SI. This latter step helps reducing correlated noise, as for successive spectra different camera pixels are exposed which precludes amplification of small gain normalization errors.

To practically implement the energy-offset during SI acquisition, four possibilities are available in a modern GIF quantum energy filter [17]: TEM high tension (HT) offset, prism offset, prism adjust, and drift tube voltage offset. Adjusting the energy can be realized by Gatan scripting via the image filter control command (these commands can be found in the Digital Micrograph help file). In order to test the response speed of these methods, a suitable script was developed to calculate the time elapsed between initiating the command and completion of the energy offset. The results are summarized in Table 1 as the averages of more than 30 measurements, and the error bars given as the single standard deviation. The drift tube gives the fastest response among all the methods, whereas the HT offset method shows the slowest response speed. Another important factor of the accuracy of these techniques was also examined. A tentative linear relation of the energy-offset (ΔE) as a function of time (t) was programmed, and then a series of zero-loss peaks (ZLP) were recorded as a SI in accordance with this defined profile, i.e. $\Delta E = \alpha + \beta t$, as shown in Fig. S1 (a). The shift of the spectral position was then realigned by the Gatan SI plugin ('align SI by peak'). The real (experimental) energy shift has been plotted as a function of time in Fig. S1 (b) along with the zero-loss fluctuation (black curve). Obviously, the energy offset follows the ideal linearity and the discrepancy is minor either through adjusting the prism or the drift tube. More quantitative details regarding the discrepancy between the practical and predefined energy offset value ($\Delta E' - \Delta E$) are plotted in Fig. 1(a). The deviation is found to be within ± 2 channels, which is quite comparable to the level of the ZLP fluctuations. It highlights that all these methods can be used to offset the energy precisely via DM scripting. Notice that changing the prism current or the drift-tube voltage may degrade the optimal alignment condition of the GIF, thus degrading the energy resolution. To check this influence, we monitored the fluctuation of the energy resolution during an energy shift of up to 100 channels (which is sufficient for real multi-frame SI mapping) by these methods. The measurements were performed on real samples ($SrTiO_3$) by acquiring the ZLP. As shown in Fig. 1(b), shifting up to 100 channels did not degrade energy resolution both by adjusting the prism current or the drift-tube voltage. Without energy shift, the full width at half maximum (FWHM) of the ZLP mainly stayed at 0.8 eV, with small fluctuations of ± 0.1 eV. By applying an energy shift via adjusting the prism current and the drift-tube voltage, the FWHM of the ZLP remained in the range of 0.7 − 0.9 eV. Finally, a more practical question is whether in a later multi-frame energy-offset SI acquisition we have to acquire simultaneously low-loss SIs for the energy-offset correction. To address this question, we compared spectra of the energy-offset SI in which the energy offsets were corrected either by simultaneously acquiring zero-loss spectra (Fig. S2a) or by the ideal defined energy offset function (Fig. S2b). As demonstrated by Fig. S2, the two methods give equivalent results if we compare the final spectra. It highlights that the multi-frame energy-offset core-loss SIs can be directly realigned according to the stored offset values instead of the additional low-loss SIs as normally used in Dual-EELS routines. This significantly reduces the final data size (by almost one half) and speeds up the SI acquisition, which is particularly useful in the acquisition of large datasets and for materials prone to irradiation damage.

Table 1
Summary of methods for energy-offset in Gatan quantum energy filters and corresponding response speed. The error bars give the single standard deviation of more than 30 measurements.

Method	Response speed (ms)
Prism offset	59.5 ± 5.8
Prism adjust	57.0 ± 3.7
Drift tube	2.8 ± 0.7
HT offset	510.7 ± 64.8

2.2. Samples and post-data processing

As examples to explore these methods, $SrTiO_3$ bulk material and 2-dimensional Sr-doped La_2CuO_4 thin films on $LaSrAlO_4$ were selected. The epitaxial deposition of Sr-doped La_2CuO_4 by oxide molecular beam epitaxy has been described by Baiutti et al. [18]. TEM specimens were prepared by a standard procedure which in-